IMPACT OF MAGNETIC FIELD IN RADIATIVE FLOW OF CASSON NANOFLUID WITH HEAT AND MASS FLUXES

Tariq HUSSAIN[1,*], Shafqat HUSSAIN[1] and Tasawar HAYAT[2,3]

[1]Department of Mathematics, Faculty of Computing, Capital University of Science & Technology, Islamabad 44000, Pakistan
[2]Department of Mathematics, Quaid-I-Azam University, Islamabad 44000, Pakistan
[3]NAAM Research Group, Faculty of Science, King Abdulaziz University, Jeddah 21589, Saudi Arabia
[*]Corresponding author email: zartotariq@yahoo.com

The purpose of present article is to examine the influences of heat and mass fluxes in the magnetohydrodynamic (MHD) flow of Casson nanofluid by an exponentially stretching sheet. Formulation and analysis is presented when thermal radiation and viscous dissipation are taken into account. Transformation technique is adopted for the reduction of PDE systems to ODE systems. Both analytic and numerical solutions of dimensionless velocity, temperature and nanoparticle concentration fields are developed. The impacts of sundry parameters on the velocity, temperature and nanoparticle concentration profiles are plotted and discussed. The values of skin-friction coefficient are obtained numerically. It is found that an increase in the values of Casson parameter reduced the skin-friction coefficient while it enhances for larger Hartman number.

Keywords: *Magnetic field; Nanoparticles; Casson fluid; Viscous dissipation; Heat mass fluxes.*

1. Introduction

There are several materials like yoghurt, ice, cosmetic products, plastic polymers, fossil fuels, blood at low shear rate, egg yolk, ice cream etc. which differ from viscous liquids due to their diverse rheological characteristics [1]. Such fluids are known as the non-Newtonian fluids and these have more importance in engineering and industry. The rheological properties of non-Newtonian fluids have achieved the special attention of recent researchers. Navier-Stokes equations are not adequate to characterize the rheology of non-Newtonian materials. Also only one constitutive relationship is inadequate to explore the properties of non-Newtonian liquids. That is why various models of non-Newtonian materials have been suggested. There is one amongst these known as the Casson fluid model [2-6].

Recently thermal scientists have developed a new mechanism just to enhance the thermal conductivity of ordinary base fluids through addition of nanoparticles. Many heat transfer fluids like engine oil, ethylene glycol and water have very limited heat transfer abilities due to their low thermal characteristics. The nanofluids are the homogeneous mixture of nanoparticles and base fluid. The nanofluids have pivotal role in transportation, nuclear reactors, electronic equipment etc. Nanofluids may also be useful in biomedical applications like wound treatment, cancer therapy, safer surgery and many others. Choi [7] initially verified experimentally that the presence of nanoparticles dramatically enhanced the thermal conductivity of ordinary base liquids. Buongiorno [8] provided a model of nanofluid flow based on the Brownian motion and thermophoresis. Later different investigations have been made regarding nanofluid flows through diverse aspects and conditions [9-20].

The radiative heat transfer has superficial role in hypersonic fights, space vehicles, nuclear power plants, gas cooled nuclear reactors, gas turbines etc. Turkyilmazoglu [21] investigated the impact of thermal

radiation in the unsteady flow of viscous fluid with variable viscosity. Lin et al. [22] discussed the radiation effects on Marangoni convection non-Newtonian nanofluid in the presence of variable thermal conductivity. Radiative heat transfer in viscous nanofluid flow over a stretched sheet with velocity slip and temperature jump has been analytically reported by Zheng et al. [23]. Buoyancy effect in MHD flow of nanofluid in the presence of the thermal radiation has been numerically examined by Rashidi et al. [24]. Shehzad et al. [25] provides the series solution of Jeffrey nanofluid flow subject to thermal radiation, Brownian motion and thermophoresis effects.

The objective of present article is to investigate the impact of an applied magnetic field in two-dimensional boundary layer flow of Casson nanofluid past an exponentially stretching sheet. The role of thermal radiation is taken into account. Rosseland's approximation for thermal radiation is employed. Effects of viscous dissipation are also present. We imposed the prescribed heat and nanoparticle concentration flux conditions which are more realistic than the constant surface temperature and nanoparticle concentration conditions. Both numerical and analytical solutions have been developed through implementation of shooting technique and homotopy analysis method [26-30]. Impacts of physical parameters on the velocity, temperature and nanoparticle concentration fields are plotted and examined carefully. The skin friction coefficient for different values of Hartman number and Casson parameter has been computed and analyzed.

2. Problems statement

We consider the magnetohydrodynamic (MHD) laminar flow of Casson nanofluid induced by an exponentially stretching sheet. The nanofluid model with thermophoresis and Brownian motion effects is taken into consideration. A non-uniform magnetic field $B(x)=B_0\, exp(x/2L)$ is applied in the y-direction. Induced magnetic field for small magnetic Reynolds number is neglected. Thermal radiation and viscous dissipation are included in energy expression. We imposed the heat and mass flux conditions at the surface of the sheet. The resulting boundary layer equations can be put into the following fashion:

$$\frac{\partial u}{\partial x}+\frac{\partial v}{\partial y}=0, \tag{1}$$

$$u\frac{\partial u}{\partial x}+v\frac{\partial u}{\partial y}=\left(1+\frac{1}{\beta}\right)\frac{\partial^2 u}{\partial y^2}-\frac{\sigma B(x^2)}{\rho_f}u, \tag{2}$$

$$u\frac{\partial T}{\partial x}+v\frac{\partial T}{\partial y}=\alpha\frac{\partial^2 T}{\partial y^2}+\tau\left(D_B\frac{\partial C}{\partial y}\frac{\partial T}{\partial y}+\frac{D_T}{T_\infty}\left(\frac{\partial T}{\partial y}\right)^2\right)$$

$$+\frac{\nu}{C_p}\left(1+\frac{1}{\beta}\right)\left(\frac{\partial u}{\partial y}\right)^2, \tag{3}$$

$$u\frac{\partial C}{\partial x}+v\frac{\partial C}{\partial y}=D_B\frac{\partial^2 C}{\partial y^2}+\frac{D_T}{T_\infty}\frac{\partial^2 T}{\partial y^2}, \tag{4}$$

with the boundary conditions

$$u=u_w(x)=U_0\exp\left(\frac{x}{2L}\right),\quad v=0 \text{ at } y=0, \tag{5}$$

$$u \to 0,\ v \to 0 \text{ as } y \to \infty.$$

The boundary conditions for the prescribed heat flux (PHF) and prescribed concentration flux (PCF) are imposed as follows:

$$\text{PHF}: \ \frac{\partial T}{\partial y} = -\frac{T_0}{k}\sqrt{\frac{U_0}{2\nu L}}e^{\frac{Ax}{2L}} \text{ at } y = 0 \text{ and } T \to T_\infty \text{ when } y \to \infty, \tag{6}$$

$$\text{PCF}: \ \frac{\partial C}{\partial y} = -\frac{C_0}{D_B}\sqrt{\frac{U_0}{2\nu L}}e^{\frac{Bx}{2L}} \text{ at } y = 0 \text{ and } C \to C_\infty \text{ when } y \to \infty. \tag{7}$$

In above expressions u and v are the velocity components in the $x-$ and $y-$directions, ν the kinematic viscosity, β the Casson parameter, ρ_f the density of fluid, σ the electrical conductivity, α the thermal diffusivity, $\tau = \frac{(\rho c)_p}{(\rho c)_f}$ the ratio of nanoparticle heat capacity and the base fluid heat capacity, ν the kinematic viscosity, C_p the specific heat, D_B the Brownian diffusion coefficient, D_T the thermophoretic diffusion coefficient, k the thermal conductivity, T_0 and C_0 the reference temperature and nanoparticle concentration and T_∞ and C_∞ the ambient fluid temperature and concentration, respectively.

The radiative heat flux q_r through Rosseland approximation can be expressed as $q_r = -\frac{4\sigma^*}{3\chi}\frac{\partial T^4}{\partial y}$. We assumed a small temperature differences within the fluid flow in such a manner that T^4 can be defined as a linear function of temperature. Expanding T^4 about T_∞ and retaining only the terms upto $T - T_\infty$ we have $T^4 = T_\infty^4 + 4T_\infty^3(T - T_\infty) + 6T_\infty^2(T - T_\infty)^2 + \cdots$ [21,22] and now Eq. (3) yields

$$u\frac{\partial T}{\partial x} + v\frac{\partial T}{\partial y} = \alpha\frac{\partial^2 T}{\partial y^2} + \tau\left(D_B\frac{\partial C}{\partial y}\frac{\partial T}{\partial y} + \frac{D_T}{T_\infty}\left(\frac{\partial T}{\partial y}\right)^2\right)$$
$$+\frac{\nu}{C_p}\left(1+\frac{1}{\beta}\right)\left(\frac{\partial u}{\partial y}\right)^2 + \frac{16\sigma^* T_\infty^3}{3\rho c_p \chi}\frac{\partial^2 T}{\partial y^2}. \tag{8}$$

The similarity transformations may be represented as follows:

$$\eta = y\sqrt{\frac{U_0}{2\nu L}}\exp\left(\frac{x}{2L}\right),\ u = U_0\exp\left(\frac{x}{2L}\right)f'(\eta),\ v = -\sqrt{\frac{\nu U_0}{2L}}\exp\left(\frac{x}{2L}\right)\left(f(\eta) + \eta f'(\eta)\right),$$
$$T = T_\infty + \frac{T_0}{k}\sqrt{\frac{U_0}{2\nu L}}e^{\frac{Ax}{2L}}\theta(\eta),\ C = C_\infty + \frac{C_0}{D_B}\sqrt{\frac{U_0}{2\nu L}}e^{\frac{Bx}{2L}}\phi(\eta). \tag{9}$$

Dimensionless forms of linear momentum, energy and concentration become

$$\left(1+\frac{1}{\beta}\right)f''' + ff'' - 2f'^2 - M^2 f' = 0, \tag{10}$$

$$\left(1+\frac{4}{3}Rd\right)\theta'' + \Pr f\theta' - \Pr Af'\theta + \Pr Nb\theta'\phi' + \Pr Nt\theta'^2 + \Pr Ec\left(1+\frac{1}{\beta}\right)f''^2 = 0, \tag{11}$$

$$\phi'' + \Pr Lef\phi' - \Pr LeBf'\phi + \left(N_t / N_b\right)\theta'' = 0, \tag{12}$$

$$f=0,\quad f'=1,\quad \theta'=-1,\ \phi'=-1\quad \text{at}\ \eta=0,$$
$$f'\to 0,\quad \theta\to 0,\ \phi\to 0\quad \text{as}\ \eta\to\infty, \tag{13}$$

in which $M^2=2\sigma B_0^2 L/\rho_f U_0$ the magnetic parameter, $\Pr=\nu/\alpha$ the Prandtl number, $Le=\nu/D_B$ the Lewis number, $Nb=(\rho c)_p D_B(C-C_0)/(\rho c)_f\nu$ the Brownian motion parameter, $Nt=(\rho c)_p D_T(T-T_0)/(\rho c)_f\nu T_0$ the thermophoresis parameter, $Rd=4\sigma^* T_\infty^3/k\chi$ the thermal radiation parameter and condition (1) is identically satisfied. The presented analysis can be reduced to viscous fluid case when $\beta\to\infty$.

The skin friction coefficient is

$$\sqrt{2\,\mathrm{Re}_x}\,C_{fx}=\left(1+\frac{1}{\beta}\right)f''(0)), \tag{14}$$

where $\mathrm{Re}_x=u_w(x)L/\nu$ denotes the local Reynolds number.

3. Discussion

Here the problems subjected to velocity, temperature and nanoparticle concentration fields are computed by shooting technique and homotopy analysis method for the numerical and approximate solutions, respectively. Thus Figs. 1 and 2 are plotted to investigate the impacts of Hartman number M and Casson parameter β on the dimensionless velocity distribution $f'(\eta)$. Fig. 2 shows the variations in velocity $f'(\eta)$ for different values of Hartman number when $\beta=0.2$. It is noted that the velocity profile is enhanced for decreasing values of Hartman number. The velocity is lower when $M=2$ and it starts to increase as the values of M become smaller. Obviously the Hartman number is through Lorentz force and this Lorentz force is weaker for smaller Hartman number and stronger for larger M. Here Lorentz force offers a resistance to fluid flow and due to stronger Lorentz force, the velocity is decreased for larger Hartman number. The fluid velocity and momentum boundary layer thickness are reduced for larger values of Casson parameter when $M=0.6$ (see Fig. 2).

Fig. 3 illustrates the variations in temperature field $\theta(\eta)$ for different values of Prandtl number $\Pr$. An increase in Prandtl number shows lower temperature and thinner thermal boundary layer thickness. Prandtl number possesses thermal diffusivity. Thermal diffusivity has a major role in Prandtl number. Weaker thermal diffusivity appeared when we enhance the values of Prandtl number and such weaker thermal diffusivity is responsible for a reduction in temperature. Influence of Eckert number Ec on the temperature field is reported in Fig. 4. In fact Eckert number appeared here due to presence of viscous dissipation. The viscous dissipation term is absent when $Ec=0$. Here it is studied that the temperature field and thermal boundary layer thickness are higher for larger values of Eckert number. Clearly Eckert number depends on the kinetic energy and kinetic energy is enhanced when the values of Eckert number increase. Such increase in kinetic energy leads to thicker thermal boundary layer thickness. Figs. 5 and 6 explore the characteristics of Brownian motion parameter N_b and thermophoresis parameter N_t on the temperature profile. We observed that the larger values of Brownian motion parameter N_b and thermophoresis parameter N_t enhance the temperature and thermal boundary layer thickness

remarkably. Physically the Brownian motion and thermophoresis parameters appeared due to presence of nanoparticles. The presence of nanoparticles gives rise to thermal conductivity of liquid. The thermal conductivity of liquid is higher when we use the larger values of Brownian motion and thermophoresis parameters and this stronger thermal conductivity corresponds to higher temperature. It is examined from Fig. 7 that the temperature is enhanced when we use larger values of thermal radiation parameter Rd. Thus more heat is absorbed by the fluid when thermal radiation is present due to which temperature enhances. Fig. 8 depict that the temperature is lower for hydrodynamic flow $(M=0)$ when compared with hydromagnetic flow $(M>0)$. The Lorentz force is absent when we consider the hydrodynamic flow and sure it appears in the case of hydromagnetic flow. The Lorentz force resists the fluid flow due to which more heat is produced in the liquid and higher temperature is observed.

Figs. 9-13 present the changes in nanoparticle concentration profile $\phi(\eta)$ for different values of Prandtl number $\Pr$, Eckert number Ec, thermophoresis and Brownian motion parameters N_t and N_b and Lewis number Le. Fig. 9 reports that an increase in the values of Prandtl number creates a reduction in nanoparticle concentration and its associated boundary layer thickness. The nanoparticle concentration is decreased firstly when we enhance the values of Eckert number but at $\eta=1.2$ it starts to increase (see Fig. 10). The variations in nanoparticle concentration field for different values of thermophoresis parameter and Brownian motion parameter are studied in the Figs. 11 and 12. Here we noticed that the higher values of thermophoresis parameter correspond to larger nanoparticle concentration while on the other hand it decreases when we enhance the values of Brownian motion parameter. Fig. 13 illustrates the influence of Lewis number on nanoparticle concentration profile. The nanoparticle concentration field is decreased gradually for the increasing values of Lewis number. Brownian diffusion coefficient appeared in Lewis number and it is weaker for larger Lewis number. Due to such weaker Brownian diffusion coefficient, nanoparticle concentration field is lower. Table 1 shows the comparison between homotopic and numerical solutions for different values of Casson parameter β and Hartman number M. This Table witnesses that our numerical and homotopic solutions are in an excellent agreement.

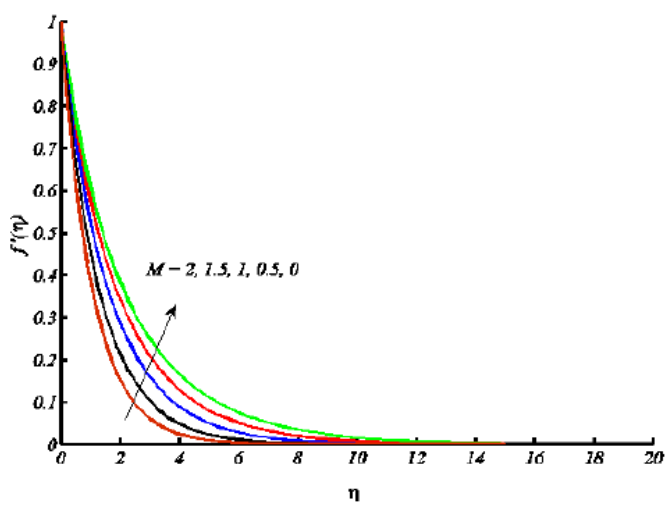

Fig. 1: Impact of M on velocity field $f'(\eta)$ vs η when $\beta=0.2$.

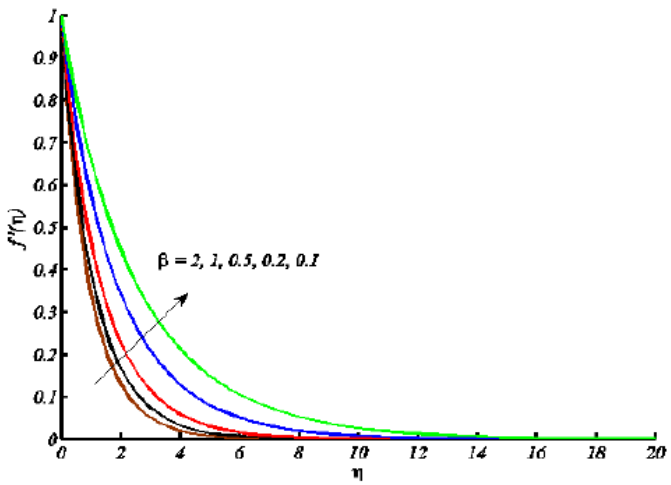

Fig. 2: Impact of β on velocity field $f'(\eta)$ vs η when $M = 0.6$.

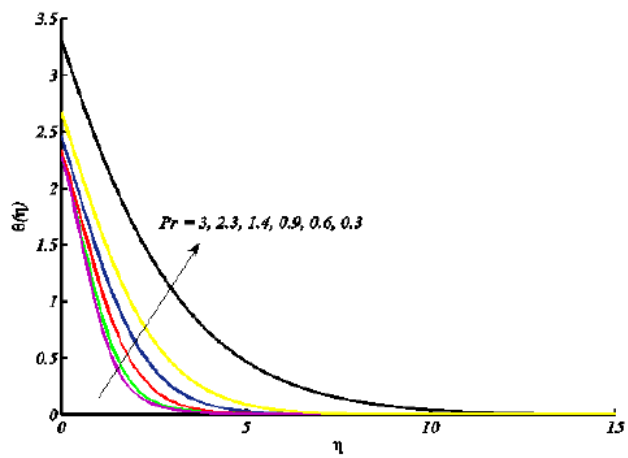

Fig. 3: Impact of $\Pr$ on temperature field $\theta(\eta)$ vs η when $M = 0.5$, $\beta = 0.2 = Rd$, $Ec = 1.0$, $Le = 0.5$, $N_t = 0.1$ and $N_b = 1.0$.

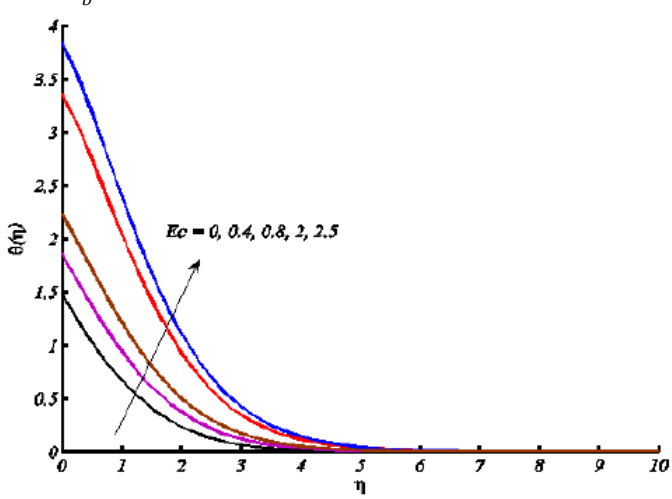

Fig. 4: Impact of Ec on temperature field $\theta(\eta)$ vs η when $M = 0.5$, $\beta = 0.2 = Rd$, $\Pr = 1.0$, $Le = 0.5$, $N_t = 0.1$ and $N_b = 1.0$.

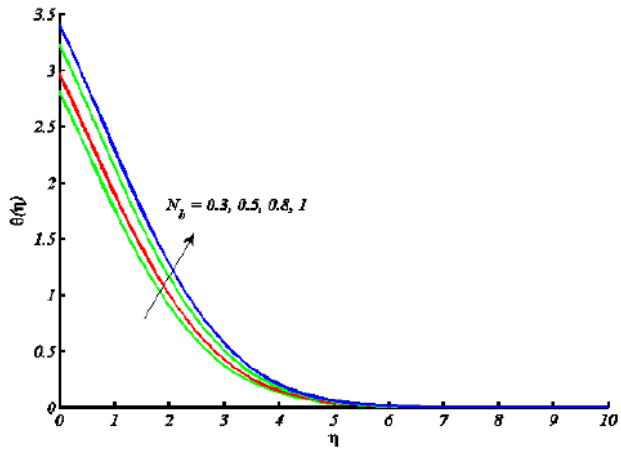

Fig. 5: Impact of N_b on temperature field $\theta(\eta)$ vs η when $M = 0.5$, $\beta = 0.2 = Rd$, $\Pr = 1.0$, $Le = 0.5$, $N_t = 0.1$ and $Ec = 1.0$.

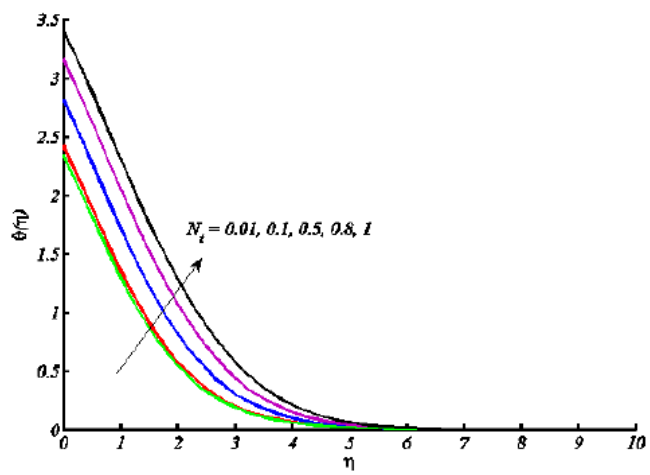

Fig. 6: Impact of N_t on temperature field $\theta(\eta)$ vs η when $M = 0.5$, $\beta = 0.2 = Rd$, $\Pr = 1.0$, $Le = 0.5$, $N_b = 1.0$ and $Ec = 1.0$.

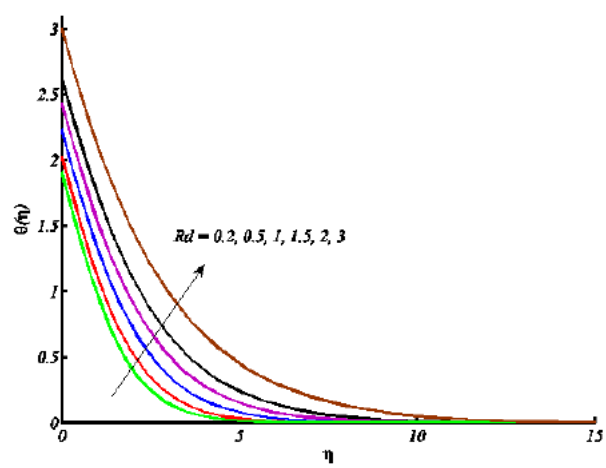

Fig. 7: Impact of Rd on temperature field $\theta(\eta)$ vs η when $M = 0.5$, $\beta = 0.2$, $\Pr = 1.0$, $Le = 0.5$, $N_t = 0.1$, $N_b = 1.0$ and $Ec = 1.0$.

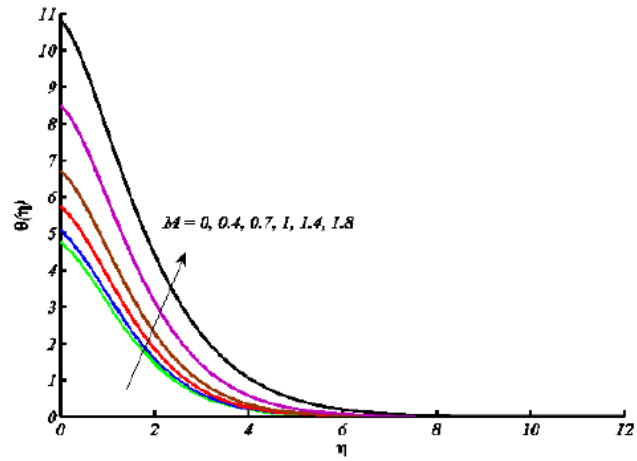

Fig. 8: Impact of M on temperature field $\theta(\eta)$ vs η when $\beta = 0.2 = Rd$, $\Pr = 1.0$, $Le = 0.5$, $N_t = 0.1$, $N_b = 1.0$ and $Ec = 1.0$.

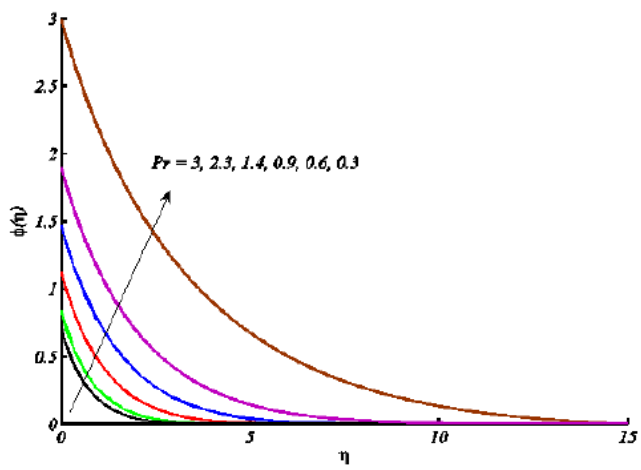

Fig. 9: Impact of $\Pr$ on nanoparticle concentration field $\phi(\eta)$ vs η when $M = 0.5$, $\beta = 0.2 = Rd$, $Le = 0.5$, $N_t = 0.1$, $N_b = 1.0$ and $Ec = 1.0$.

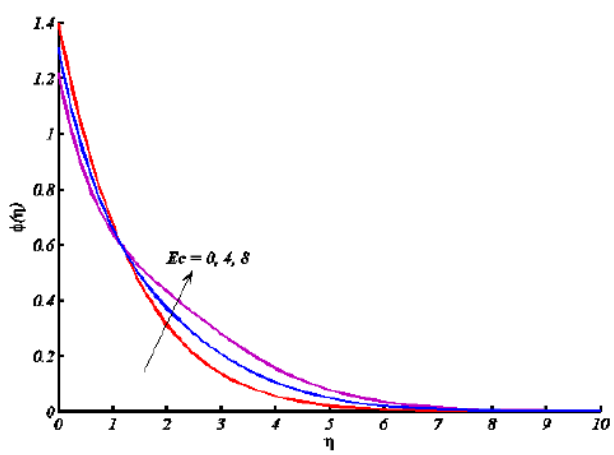

Fig. 10: Impact of Ec on nanoparticle concentration field $\phi(\eta)$ vs η when $M = 0.5$, $\beta = 0.2 = Rd$, $\Pr = 1.0$, $Le = 0.5$, $N_t = 0.1$ and $N_b = 1.0$.

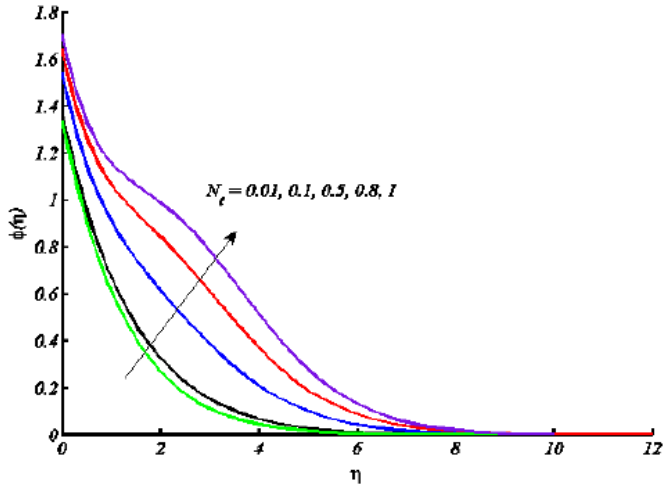

Fig. 11: Impact of N_t on nanoparticle concentration field $\phi(\eta)$ vs η when $M = 0.5$, $\beta = 0.2 = Rd$, $\Pr = 1.0$, $Le = 0.5$, $Ec = 1.0$ and $N_b = 1.0$.

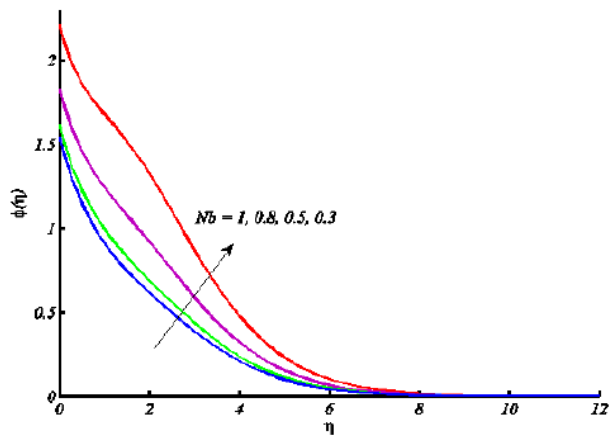

Fig. 12: Impact of N_b on nanoparticle concentration field $\phi(\eta)$ vs η when $M = 0.5$, $\beta = 0.2 = Rd$, $\Pr = 1.0$, $Le = 0.5$, $Ec = 1.0$ and $N_t = 0.5$.

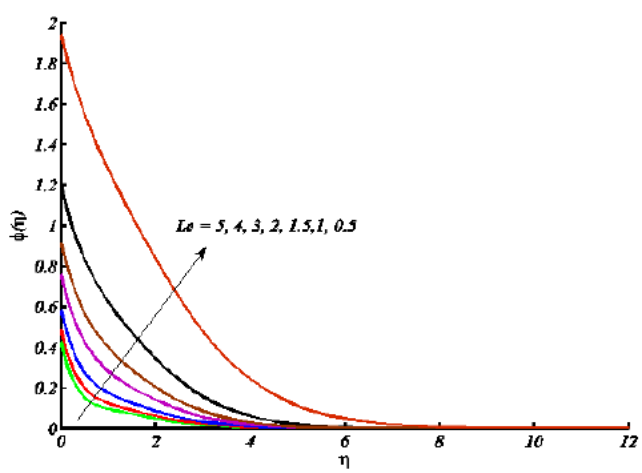

Fig. 13: Impact of Le on nanoparticle concentration field $\phi(\eta)$ vs η when $M = 0.5$, $\beta = 0.2 = Rd$, $\Pr = 1.0$, $Ec = 1.0$ and $N_t = 0.1 = N_b$.

Table 1: Numerical values of skin friction coefficient $(1+1/\beta)f''(0)$ for different values of β and M.

β	M	$-(1+1/\beta)f''(0)$	
		HAM solution	Numerical solution
1.0	0.6	2.00447	2.00446
1.4	0.6	1.85578	1.85577
1.7	0.6	1.78624	1.78624
2.0	0.6	1.73592	1.73592
1.5	0.0	1.65488	1.65480
1.5	0.5	1.77835	1.77834
1.5	0.8	1.95437	1.95437
1.5	1.0	2.10327	2.10325

4. Conclusions

Here we explored the impacts of thermal radiation, viscous dissipation and applied magnetic field in boundary layer flow of Casson nanofluid through heat and mass flux conditions. The main conclusions of this work can be summarized through the following points.

- The velocity field $f'(\eta)$ is increased for larger values of Hartman number M and Casson parameter β. Here $M=0$ leads to hydrodynamic flow while $\beta \to \infty$ corresponds to viscous fluid flow.
- Temperature $\theta(\eta)$ is enhanced for larger Eckert number Ec. Here an increase in Eckert number corresponds to higher kinetic energy due to which larger temperature is noticed.
- An increase in the values of Brownian motion and thermophoresis parameter leads to an enhancement in the temperature profile and thermal boundary layer thickness.
- Thermal boundary layer thickness is more in presence of thermal radiation.
- The nanoparticle concentration field is enhanced dramatically corresponding to the increasing values of thermophoresis parameter but it reduces for larger Brownian motion parameter.

Nomenclature

u,v,x,y	velocity components along x and y [ms^{-1}]	$B(x)$	variable magnetic field [$kgs^{-2}A^{-1}$]
β	Casson parameter [-]	σ	electrical conductivity [$s^3A^2kg^{-1}m^{-3}$]
B_0	constant magnetic field [$kgs^{-2}A^{-1}$]	ρ_f	density of fluid [kgm^{-3}]
T	Temperature [K]	τ	ratio of nanoparticle heat capacity [-]
D_B	Brownian diffusion coefficient[$kgm^{-1}s^{-1}$]	D_T	thermophoretic diffusion coefficient [$kgm^{-1}s^{-1}K^{-1}$]
ν	kinematic viscosity [m^2s^{-1}]	C_p	specific heat [m^2s^{-2}]

C	nanoparticle concentration [-]	u_w	stretching velocity [ms^{-1}]
U_0	reference velocity [ms^{-1}]	T_0	reference temperature [K]
C_0	reference concentration [-]	k	thermal conductivity [$WK^{-1}m^{-1}$]
A	temperature exponential coefficient [-]	B	concentration exponential coefficient [-]
q_r	radiative heat flux [-]	σ^*	Steffan-Boltzman constant [-]
χ	mean absorption coefficient [-]	L	reference length [-]
η	similarity variable [-]	f	dimensionless velocity [-]
θ	dimensionless temperature [-]	ϕ	dimensionless concentration [-]
M	magnetic parameter [-]	Pr	Prandtl number [-]
Le	Lewis number [-]	Ec	Eckert number [-]
Rd	radiation parameter [-]	Nt	thermophoretic parameter [-]
Nb	Brownian motion parameter [-]	Re_x	local Reynolds number [-]
C_{fx}	skin-friction coefficient [-]		

References

[1] Dalir, N., Dehsara, M., Nourazar, S.A., Entropy analysis for magnetohydrodynamic flow and heat transfer of a Jeffrey nanofluid over a stretching sheet, *Energy*, 79 (2015), pp. 351-362, DOI:10.1016/j.energy.2014.11.021

[2] Boyd, J., Buick, J.M., Green, S., Analysis of the Casson and Carreau-Yasuda non-Newtonian blood models in steady and oscillatory flow using the lattice Boltzmann method, *Phys. Fluids*, 19 (2007), pp. 93-103, DOI.org/10.1063/1.2772250

[3] Hayat, T., Shehzad, S.A., Alsaedi, A., Alhothuali, M.S., Mixed convection stagnation point flow of Casson fluid with convective boundary conditions, *Chin. Phys. Lett.*, 29 (2012), 11, pp. 114704

[4] Mustafa, M., Hayat, T., Pop, I., Hendi, A.A., Stagnation-point flow and heat transfer of a Casson fluid towards a stretching sheet, *Z Naturforsch. A*, 67a (2012), pp. 70-76, DOI:10.5560/ZNA.2011-0057

[5] Mukhopadhyay, S., Casson fluid flow and heat transfer over a nonlinearly stretching surface, *Chin. Phys. B*, 22 (2013), 7, pp. 074701, DOI: 10.1088/1674-1056/22/7/074701

[6] Hayat, T., Farooq, M., Alsaedi, A., Thermally stratified stagnation point flow of Casson fluid with slip conditions, *Int. J. Numer. Methods Heat Fluid Flow*, 25 (2015), 4, pp. 724-748, DOI: http://dx.doi.org/10.1108/HFF-05-2014-0145

[7] Choi, S.U.S., Enhancing thermal conductivity of fluids with nanoparticles, in: The Proceedings of the 1995 ASME International Mechanical Engineering Congress and Exposition, *San Francisce, USA, ASME, FED 231/ MD*, 66 (1995), pp. 99-105

[8] Buongiorno, J., Convective transport in nanofluids, *J. Heat Transfer-Trans. ASME*, 128 (2006), 3, pp. 240-250, DOI: 10.1115/1.2150834

[9] Turkyilmazoglu, M., Exact analytical solutions for heat and mass transfer of MHD slip flow in nanofluids, *Chem. Eng. Sci.*, 84 (2012), pp. 182-187, DOI:10.1016/j.ces.2012.08.029

[10] Ibrahim, W., Shankar, B., Nandeppanavar, M.M., MHD stagnation point flow and heat transfer due to nanofluid towards a stretching sheet, *Int. J. Heat Mass Transfer*, 56 (2013), 1-2, pp. 1-9, DOI:10.1016/j.ijheatmasstransfer.2012.08.034

[11] Makinde, O.D., Khan, W.A., Khan, Z.H., Buoyancy effects on MHD stagnation point flow and heat transfer of a nanofluid past a convectively heated stretching/shrinking sheet, *Int. J. Heat Mass Transfer*, 62 (2013), pp. 526-533, DOI:10.1016/j.ijheatmasstransfer.2013.03.049
[12] Sheikholeslami, M., Ganji, D.D., Three dimensional heat and mass transfer in a rotating system using nanofluid, *Powder Technology*, 253 (2014), pp. 789-796, DOI:10.1016/j.powtec.2013.12.042
[13] Turkyilmazoglu, M., A note on the correspondence between certain nanofluid flows and standard fluid flows, *J. Heat Transfer-Trans. ASME*, 137 (2015), 2, pp. 024501, DOI: 10.1115/1.4028807
[14] Garoosi, F., Rohani, B., Rashidi, M.M., Two-phase mixture modeling of mixed convection of nanofluids in a square cavity with internal and external heating, *Powder Technology*, 275 (2015), pp. 304-321, DOI:10.1016/j.powtec.2015.02.015
[15] Zhang, C., Zheng, L., Zhang, X., Chen, G., MHD flow and radiation heat transfer of nanofluids in porous media with variable surface heat flux and chemical reaction, *Appl. Math. Modell.*, 39 (2015), 1, pp. 165-181, DOI:10.1016/j.apm.2014.05.023
[16] Hayat, T., Hussain, T., Shehzad, S.A., Alsaedi, A., Flow of Oldroyd-B fluid with nanoparticles and thermal radiation, *Appl. Math. Mech.*, 36 (2015), 1, pp. 69-80, DOI: 10.1007/s10483-015-1896-9
[17] Hussain, T., Hayat, T., Shehzad, S.A., Alsaedi, A., Chen, B., A model of solar radiation and Joule heating in flow of third grade nanofluid, *Z Naturforsch. A*, 70 (2015), pp. 177-184.
[18] Sheikholeslami, M., Hatami, M., Domairry, G., Numerical simulation of two phase unsteady nanofluid flow and heat transfer between parallel plates in presence of time dependent magnetic field, *J. Taiwan Inst. Chem. Eng.*, 46 (2015), pp. 43-50, DOI:10.1016/j.jtice.2014.09.025
[19] Lin, Y., Zheng, L., Zhang, X., Ma, L., Chen, G., MHD pseudo-plastic nanofluid unsteady flow and heat transfer in a finite thin film over stretching surface with internal heat generation, *Int. J. Heat Mass Transfer*, 84 (2015), pp. 903-911, DOI:10.1016/j.ijheatmasstransfer.2015.01.099
[20] Abbasi, F.M., Hayat, T., Ahmad, B., Peristalsis of silver-water nanofluid in the presence of Hall and Ohmic heating effects: Applications in drug delivery, *J. Mol. Liq.*, 207 (2015), pp. 248-255, DOI:10.1016/j.molliq.2015.03.042
[21] Turkyilmazoglu, M., Thermal radiation effects on the time-dependent MHD permeable flow having variable viscosity, *Int. J. Thermal Sci.*, 50 (2011), 1, pp. 88-96, doi:10.1016/j.ijthermalsci.2010.08.016
[22] Lin, Y., Zheng, L., Zhang, X., Radiation effects on Marangoni convection flow and heat transfer in pseudo-plastic non-Newtonian nanofluids with variable thermal conductivity, *Int. J. Heat Mass Transfer*, 77 (2014), pp. 708-716, DOI:10.1016/j.ijheatmasstransfer.2014.06.028
[23] Zheng, L., Zhang, C., Zhang, X., Zhang, J., Flow and radiation heat transfer of a nanofluid over a stretching sheet with velocity slip and temperature jump in porous medium, *Journal of Franklin Institute*, 350 (2013), 5, pp. 990-1007, DOI:10.1016/j/jfranklin.2013.01.022
[24] Rashidi, M.M., Ganesh, N.V., Hakeem, A.K.A., Ganga, B., Buoyancy effect on MHD flow of nanofluid over a stretching sheet in the presence of thermal radiation, *J. Mol. Liq.*, 198 (2014), pp. 234-238, doi:10.1016/j.molliq.2014.06.037
[25] Shehzad, S.A., Hayat, T., Alsaedi, A., Obid, M.A., Nonlinear thermal radiation in three-dimensional flow of Jeffrey nanofluid: A model for solar energy, *Appl. Math. Comput.*, 248 (2014), pp. 273-286, doi:10.1016/j.amc.2014.09.091
[26] Liao, S.J., Homotopy analysis method in nonlinear differential equations, *Springer & Higher Education Press, Heidelberg*, 2012
[27] Turkyilmazoglu, M., Solution of the Thomas-Fermi equation with a convergent approach, *Commun. Nonlinear Sci. Numer. Simulat.*, 17 (2012), 11, pp. 4097-4103, DOI:10.1016/j.cnsns.2012.01.030
[28] Hayat, T., Shehzad, S.A., Qasim, M., Obaidat, S., Flow of a second grade fluid with convective boundary conditions, *Thermal Sci.*, 15 (2011), S2, pp. 253-261, DOI: 10.2298/TSCI101014058H
[29] Abbasi, F.M., Shehzad, S.A., Hayat, T., Alsaedi, A., Obid, M.A., Influence of heat and mass flux conditions in hydromagnetic flow of Jeffrey nanofluid, *AIP Adv.*, 5 (2015), 037111, DOI: http://dx.doi.org/10.1063/1.4914549
[30] Hayat, T., Imtiaz, M., Alsaedi, A., MHD flow of nanofluid with homogenous-hetreogenous reactions and velocity slip, *Thermal Sci.*, DOI: 10.2298/TSCI140922067H

Paper submitted: July 12, 2015
Paper revised: February 24, 2016
Paper accepted: March 3, 2016